Biomass Conversion and Biorefinery
https://doi.org/10.1007/s13399-023-04997-x

ORIGINAL ARTICLE

Production of fermentable sugar, ethanol, D-lactic acid, and biochar from starch-rich traditional Chinese medicine decoction residues

Xin Gao[1] · Tingting Xu[1] · Yunlin Shi[1] · Zhongzhong Bai [1] · Jun Zhou [1] · Hongli Wu[1] · Fei Cao[1] · Ping Wei[1]

Received: 19 July 2023 / Revised: 25 September 2023 / Accepted: 9 October 2023

Abstract
Roots and stems comprise a large proportion of traditional Chinese medicines and often serve as the energy storage units of plants. However, their decoction residues still contain a significant amount of starch, and direct landfilling, incineration, or carbon disposal results in a wastage of resources. In this study, five types of starch-rich traditional Chinese medicine decoction residues (TCMDRs)c, namely, *Radix Isatidis Rhizoma Dioscoreae*, *Rhizoma Corydalis* and *Fritillaria Thunbergii*. *Radix Paeoniae Alba* were screened and hydrolyzed using amylase-glucoamylase to produce fermentable sugar. The resulting glucose yields were 87.54%, 84.51%, 85.14%, 82.55%, and 87.75%, respectively. The enzymatic hydrolysate, after flocculation-decolorization treatment, was used to produce D-lactic acid and ethanol, resulting in a concentration and yield of 121.11 g/L (0.97 g/g) and 54.17 g/L (0.49 g/g), respectively. When single or mixed starch-rich TCMDRs were directly used as feedstocks for ethanol production via simultaneous saccharification and fermentation (SSF), they exhibited similar ethanol fermentability, with yields ranging from 0.33 to 0.43 g/g. The SSF residues were thermochemically transformed into biochar with a specific surface area of 89–459 m^2/g to reduce secondary waste generation. The utilization value of starch-rich TCMDRs was significantly improved through the implementation of enzymatic hydrolysis to produce fermentable sugars, anaerobic fermentation to produce D-lactic acid and ethanol, and the utilization of fermentation residues for biochar production.

Keywords Starch-rich TCMDRs · SSF · Ethanol · D-Lactic acid · Biochar

1 Introduction

In recent years, traditional Chinese medicine (TCM) and its active ingredients have attracted significant attention for their potential anti-inflammatory [1] and antiviral effects [2], tumor growth inhibition, cancer treatment [3], and the treatment of liver disease [4, 5], atherosclerosis [6–8], and other diseases. Consequently, a substantial amount of decoction residues have been generated. Statistics show that the annual discharge of traditional Chinese medicine decoction residues (TCMDRs) in China is 60–70 million tons. TCMDRs represent a growing type of solid waste with unique properties, and their effective disposal can help reduce environmental pollution. Furthermore, the production of high-value products from TCMDRs can yield economic benefits and promote a virtuous cycle within the Chinese medicine industry.

Except for a small amount of animal-origin and mineral Chinese medicine [9], TCM primarily originates from plants, including whole plants (*Houttuynia cordata*, plantain, and other whole-grass medicine), flowers, seeds, fruits, stems, and roots. The decoction residues of TCM usually contain lignocellulose. For example, Li et al. [10] summarized the lignocellulosic components of various monomers and mixed TCM, reporting 19.3–48.0% cellulose content, 10.6–32.2% hemicellulose content, and 9.2%–42.3% lignin content. Wang et al. [11] analyzed the cellulose, hemicellulose, and lignin components in ginseng residue after decoction, revealing percentages of 49.52 ± 1.46%, 12.56 ± 0.36%, and 21.30 ± 0.02%, respectively. Polysaccharides, ginsenosides, and succinic acid were subsequently co-produced from the ginseng residue. Zhang et al. [12] examined the lignocellulose components of*Glycyrrhiza uralensis*,*Sophora flavescens*, and*Radix isatidis* after decoction, revealing approximately

✉ Hongli Wu
hlwu@njtech.edu.cn

1 College of Biotechnology and Pharmaceutical Engineering, Nanjing Tech University, 30 South Puzhu Road, Nanjing 211816, People's Republic of China

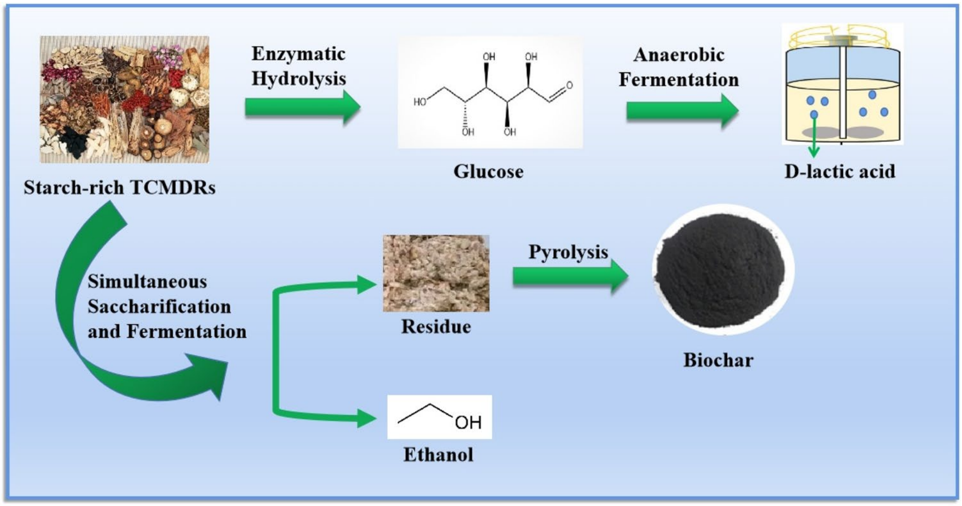

Scheme 1 Comprehensive utilization of starch-rich TCMDRs

19–28% cellulose, 15–23% hemicellulose, and 30–43% lignin. These residues can be utilized as substrates for *Penicillium oxalicum* G2 fermentation to produce cellulase. Li et al. [13] systematically measured the lignocellulose content of 40 typical TCMDRs and found that 28 types had lignocellulose content exceeding 50%, accounting for 70.0%. Notably, some rhizomatous TCMDRs were found to have high starch content. Currently, the extensive treatment of waste resources, such as starch-rich TCMDRs, involves incineration, stacking, and landfilling, all of which contribute to significant pollution and resource wastage [14, 15].

Starch-rich wastes can be converted into glucose [16], which can then be fermented to produce L-lactic acid [17], ethanol [18], succinic acid [19], and hydrogen [20]. Alternatively, they can undergo chemical catalysis to produce HMF [21], LA [22], methyl lactate [23], dehydrating sugar [24], and other bio-based platform compounds. Recently, He et al. [25] employed a hydrolysate of starch-rich solids from kitchen waste to prepare a superhydrophobic stearic acid-modified BC aerogel (S-BCA) for adsorbing cooking oil. S-BCA exhibited a significant saturated oil adsorption capacity of 48.2 g/g and demonstrated superior recyclability for at least 10 cycles, with 89% of the initial adsorption capacity retained. Additionally, Karim et al. [26] investigated and assessed the potential use of cassava peel and bagasse as alternative biodegradable food packaging materials. Furthermore, Zhang [27] and Qiao [28] prepared biochar from starch-rich food waste and used it to effectively remove tetracycline antibiotics (TCs) from water and produce electrode materials with a high specific capacitance.

However, the utilization of starch-rich TCMDRs has long been neglected because the starch content of TCMDRs is unknown and they are frequently mixed with other TCMs. Based on previous studies, we screened five types of starch-rich TCMDRs and used α-amylase and glucoamylase to produce sugars from single and mixed starch-rich TCMDRs. Following the flocculation-decolorization treatment, the enzymatic hydrolysate of mixed TCM residues could be employed for ethanol and D-lactic acid fermentation. To simplify the treatment process, we investigated simultaneous saccharification and fermentation (SSF) to produce ethanol directly using mixed starch-rich TCMDRs as raw materials for fermentation. To prevent secondary environmental damage and achieve comprehensive utilization of starch-rich TCMDRs, the residue obtained after the SSF process with ethanol was used to produce the corresponding biochar via hydrothermal carbonization, and the biochar was subsequently characterized (Scheme 1).

2 Materials and methods

2.1 Materials

Radix Isatidis (RI), *Rhizoma Dioscoreae* (RD), *Rhizoma Corydalis* (RC), *Fritillaria Thunbergii* (FT), and *Radix Paeoniae Alba* (RPA) were purchased from Anhui Bozhou Anbo Pharmaceutical Co., Ltd. α-Amylase and glucoamylase were purchased from Sigma-Aldrich. Cornstarch, amylose, yeast extract, peptone, dry corn pulp powder, bran, activated carbon, and glucose were purchased from Shanghai Aladdin Biochemical Technology Co., Ltd. All other chemical reagents were purchased from Nanjing Wanqing Chemical Glass Instrument Co., Ltd.

2.2 Biomass analysis of starch-rich TCMDRs

(1) Determination of lignocellulose components

The contents of glucan (cellulose and starch), hemicellulose, and lignin in the different TCMDRs were determined using NREL's laboratory analytical procedures [29] and basing on our previous report [24].The calculation followed the equation of the NREL method, and results for each sample were expressed as the mean of three replicates.

(2) Determination of gelatinized starch content

Based on the enzymatic liquefaction and saccharification of cornstarch, the starch components in starch-rich TCMDRs were sequentially degraded into glucose by α-amylase (EC 3.2.1.1) and glucoamylase (EC 3.2.1.3); the starch contents in TCMDRs were calculated from the determined glucose concentration. The detailed experimental procedures are referred to the "Supplementary information."

2.3 Optimization of enzymatic hydrolysis conditions and pretreatment

The enzymatic hydrolysis conditions of the starch-rich TCMDRs were optimized, and the liquefaction process remained unchanged. The effects of enzymatic hydrolysis parameters such as temperature, pH, enzyme dosage, and reaction time were evaluated using the yield of glucose. The glucose yield from starch-rich TCMDRs was calculated using the following equation:

$$\text{glucose yield (\%)} = \frac{\text{Glucose content}}{(\text{starch content} + \text{cellulose content})} \times 100$$

The flocculant $AlCl_3$ then was added to the enzymatic hydrolysate of the RI residue at a proportion of 2%, and the flocculated mixture was centrifuged for 5 h at 50 °C. The supernatant was mixed with 2 g/100 g of activated carbon and decolorized at 50 °C.

2.4 Preparation of D-lactic acid from enzymatic hydrolysate

Based on Zheng [30] et al.'s report,*Sporolactobacillus* YBS1-5 was cultured in a medium (glucose, 20.0 g; yeast extract, 2.0 g; peptone, 2.0 g; dry corn pulp powder, 5.0 g; bran 2.0 g; $MgSO_4$ 0.2 g/L; pH 7.0). The culture sealed with liquid paraffin and incubated on a shaking bed at 37 °C and 150 rpm for 16 h. Subsequently, 10% (v/v) of the culture was added to a 1-L fermentation medium (hydrolysate glucose, 125.0 g; yeast extract, 10.0 g; dry corn pulp powder, 15.0 g; $MgSO_4$, 0.5 g; $CaCO_3$, 90.0 g/L; pH 6.0) in a 2-L fermenter, which was sealed with liquid paraffin and cultured at 37 °C. Samples were collected every 24 h to measure the pH, bacterial concentration, residual glucose, and D-lactic acid yield.

A certain amount of fermentation was centrifuged at 12,000 rpm/min for 1 min, the supernatant was discarded, and the weight of wet bacteria was weighed. Calculation method of bacterial concentration:

$$\text{Bacterial concentration} = \frac{\text{Weight of wet bacteria}}{\text{Volume of fermentation}}$$

Calculation method of D-lactic acid yield:

$$\text{D} - \text{lactic acid yield}\left(\frac{\text{g[D} - \text{lactic acid]}}{\text{g}[\text{glucose}]}\right) = \frac{\text{D} - \text{lactic acid concentration}\,[\text{g/L}]}{\text{initial glucose} - \text{final glucose}\,[\text{g/L}]}$$

2.5 Preparation of ethanol from enzymatic hydrolysate or by SSF process

The decolorized hydrolysate was substituted for glucose to ferment ethanol in a 2-L fermenter. The media consisted of hydrolysate glucose (100.0 g), $CaCl_2$ (11.1 g), KH_2PO_4 (4.0 g), $MgSO_4{\cdot}7H_2O$ (0.4 g), and $(NH4)_2SO_4$ (2.0 g/L). The initial pH was 5.0, and the Angel yeast dosage was 10 g/L.

In the SSF process, starch was added to maintain an initial glucose concentration of 100 g/L, and the initial TCMDR dosage was calculated based on the starch content of the TCMDRs. Based on Silva et al. [31]'s report, the prepared fermentation media were poured into a 2-L fermenter and sterilized in a high-pressure steam sterilizer at 121 °C for 20 min. The fermenter was then removed when the temperature dropped to 95 °C. High-temperature-resistant α-amylase (40 U/g) was added, and the rotational speed was set to 500 rpm to initiate the liquefaction. An iodine chromogenic reaction was used to verify the complete liquefaction of the starch. After cooling to 37 °C, the glucoamylase (250 U/g) and Angel yeast (10 g/L) were added for the SSF process to produce ethanol.

Samples were taken at regular intervals to measure the pH, bacterial concentration, residual glucose, and ethanol yield. The following method was used to calculate the sugar alcohol conversion:

$$\text{Ethanol yield}\left(\frac{\text{g[ethanol]}}{\text{g}[\text{glucose}]}\right) = \frac{\text{ethanol concentration}\,[\text{g/L}]}{\text{initial glucose} - \text{final glucose}\,[\text{g/L}]}$$

2.6 Preparation of biochar from SSF residues

After SSF process, the ethanol fermentation residues were washed three times with deionized water, and then dried for 24 h. Based on the method of Lin and Cui [32, 33], the dried residues were thoroughly mixed with 25 mL 10% KOH solution at a mass ratio of 1:2. The mixture was heated to 800 °C at a heating rate of 10 °C/min and maintained for 4 h in a tube furnace (Lichen, SRJX-4-13, China). The pyrolyzed product was washed with deionized water until to be neutral and dried at 105 °C.

2.7 Analytical method

Glucose, xylose, arabinose, D-lactic acid, and ethanol were detected by HPLC (Shimadzu corporation, LC-20A, Japan) equipped with refractive index detector. Aminex HPX-87H column was used in column oven at 35 °C, and 5 mM H_2SO_4 was used as mobile phase with 0.6 mL/min flowing rate.

2.8 Statistical analysis

All statistical analysis was performed with the Origin 2021 package. And results for each sample were expressed as the mean of three replicates. Values are presented as the mean ± standard deviation for data.

2.9 Characterization methods

The elemental analysis, proximate analysis, scanning electron microscopy (SEM), Fourier transform infrared spectroscopy (FT-IR), X-ray, and Brunauer–Emmett–Teller (BET) analysis for SSF residues or biochar were carried out in accordance with conventional methods. The detailed experimental procedures can be found in the "Supplementary information."

3 Results and discussion

3.1 Analysis of starch content in TCMDRs and sugar production via enzymatic hydrolysis TCMDRs

Starch in TCMDRs has long been overlooked because it is often confused with cellulose in the regular NREL method [24]. For example, both Wang [19] and Jia [34] mistook the measured glucan as cellulose in *Glycyrrhiza uralensis (GU)* and *Isatis tinctoria (IT)*. Subsequently, NREL has revised its method for determining cellulosic glucan content in starch-containing samples, but the accuracy of hemicellulose and lignin was sacrificed [35]. As the utilization difficulty of starch is obviously different from that of cellulose, it is necessary to further clarify the content of starch in TCMDRs. Cellulose and starch contents were determined using amylase enzymatic hydrolysis. Based on Li [13]'s analysis of 40 typical TCM components, we carefully determined the content of starch, cellulose, hemicellulose, lignin, alcohol-soluble components, and ash in five types of starch-rich TCMDRs (RI, RD, RC, FT, and RPA) (Fig. 1). The starch content was 62.1 ± 3.05%, 81 ± 4.21%, 58.5 ± 3.67%, 67.5 ± 4.12%, and 63 ± 2.66%, respectively, which accounted for more than half of the total biomass content. The cellulose

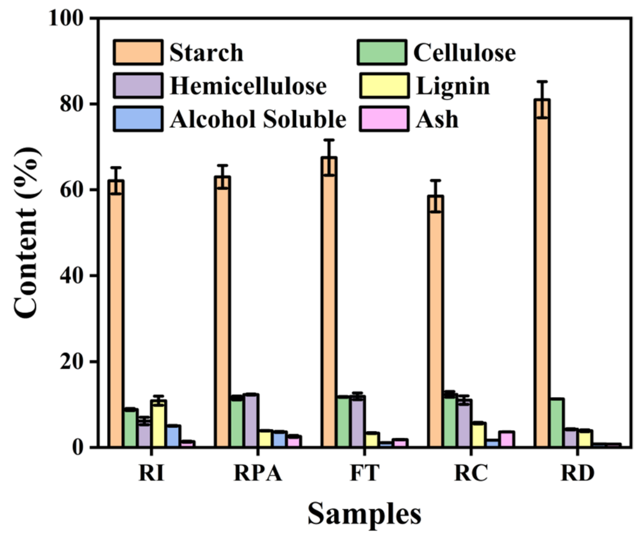

Fig. 1 Biomass analysis of starch-rich TCMDRs

content ranged from approximately 8.84 ± 0.23% to 12.37 ± 0.67%, with the total glucan content exceeding 70%. This is related to the fact that the TCMDRs itself is rhizome, which is the energy storage structure of the plant and contains a lot of starch. The alcohol-soluble component and ash contents were less than 5%. It was reported that the lignocellulose content and especially the ratio of total structural carbohydrates to lignin content (TSC/L) in cellulosic biomass feedstocks can have significant impacts on the fuel ethanol process design and economics [36]. The TCS/L ratios of five starch-rich TCMDRs were greater than 12, which were better than or comparable to those of other raw materials with bioenergy potential recommended by the DOE, such as rice straw (4.39) [37], corn straw (3.88) [38], and wheat straw (7.56) [39]. Additionally, we determined the amylose content in TCMDRs because it is better at enzymatic hydrolysis into sugar. All amylose content were less than 25% (Supplementary information Table S1), lower than that of corn starch (30.59 ± 2.79%), and more similar to the composition of potato starch [40]. This suggests that these starches differ slightly from cornstarch in terms of sugar production via enzymatic hydrolysis.

Taking the RI residue as an example, the effects of enzymatic hydrolysis parameters, such as temperature, pH, enzyme dosage, and reaction time, were evaluated. The result shows that the maximum glucose yield was 87.45% under the conditions of 60 °C, pH 5, and 250 U/g glucoamylase addition for 4 h (Supplementary information Fig. S2 and Fig. 2). These conditions were used to hydrolyze other starch-rich TCMDRs, and the glucose yields were as follows: RD, 84.51%; RC, 85.14%; FT, 82.55%; and RPA, 87.75% (Fig. 2). Furthermore, five types of starch-rich TCMDRs were mixed in equal proportions and hydrolyzed,

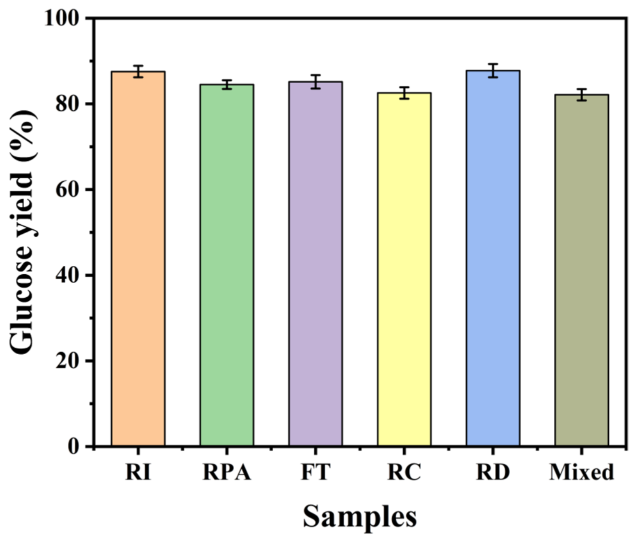

Fig. 2 Glucose yield from the single and mixed starch-rich TCMDRs via enzymatic hydrolysis

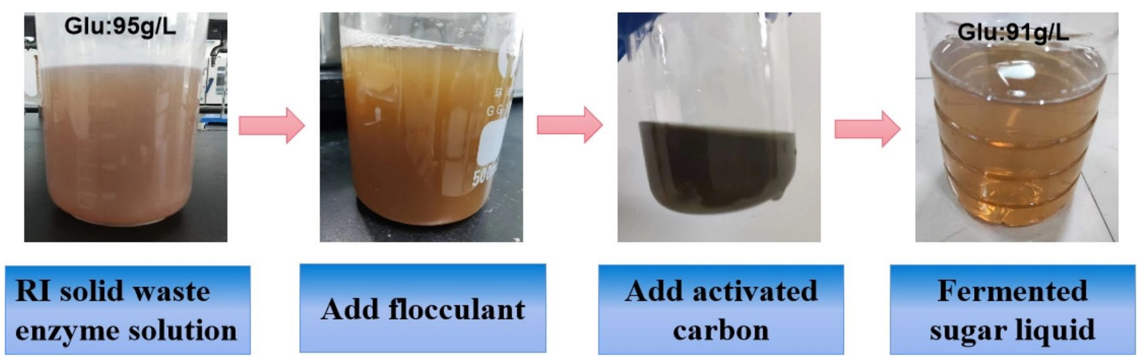

Fig. 3 Pretreatment of the enzymatic hydrolysate of the mixed starch-rich TCMDRs

resulting in glucose yields exceeding 80%. The glucose yields are lower than that of corn starch (95%) [41], which may be related to the structure and composition of the starch itself. This indicates that these starch-rich TCMDRs can be collected and hydrolyzed in a consolidated manner. Consequently, this not only overcomes the limitation of having a small quantity of decoction residues from a single TCM variety but also substantially reduces the sorting workload.

For the enzymolysis of lignocellulosic waste biomass, there are often a lot of pectin, proteins, and insoluble debris, which need to be pretreated in order to better apply to the subsequent fermentation. After the enzymatic hydrolysis of TCMDRs, it may even contain a small amount of traditional Chinese medicine active ingredients that have not been completely extracted, so further pretreatment is needed. The mixed enzymatic hydrolysate was processed using flocculant $AlCl_3$ and activated carbon (Fig. 3). This process removed macromolecules and reduced color while maximizing glucose retention. Consequently, the glucose recovery reached 96%, color was reduced by 73.3%, and a clear enzymatic hydrolysate was obtained.

3.2 Preparation of ethanol and D-lactic acid from mixed enzymatic hydrolysate via anaerobic fermentation

After decolorization, the mixed enzymatic hydrolysate can produce bio-based fuels, platform chemicals, and polymer monomers through fermentation. Compared to aerobic fermentation, anaerobic fermentation offers advantages such as facile operation, no oxygen requirement, and high yields of ethanol [42] and D-lactic acid [43]. In this study, we investigated the availability of ethanol and D-lactic acid via anaerobic fermentation of a mixed hydrolysate. Ethanol and D-lactic acid fermentation were conducted in a 2-L fermenter with initial 11% and 12.5% glucose from the mixed hydrolysate, respectively, and the results are shown in Fig. 4. During ethanol fermentation (Fig. 4a), the total consumption of glucose was reduced to 0 g/L after 16 h, and the ethanol concentration reached a peak of 54.17 g/L at 24 h. The ethanol yield was 0.49 g ethanol/g glucose, which is close to the theoretical yield of 0.51 g ethanol/g glucose [44]. This ethanol yield was higher than that of potato peel wastes (0.32g/g) [45], cassava residue (0.447g/g) [46], and oil palm trunk (0.31g/g) [47]. For D-lactic acid fermentation (Fig. 4b), all glucose was consumed after 140 h, and the D-lactic acid concentration reached a peak of 121.11 g/L at 170 h. The D-lactic acid yield was 0.97 g D-lactic acid/g glucose, which is close to the theoretical yield of 1.0 g D-lactic acid/g glucose. The D-lactic acid yield obtained from the enzymatic hydrolysate of the TCMDRs used as a carbon source substrate was even higher than that achieved through L-lactic acid fermentation from other starchy raw materials, such as potato [48], beet juice [49], sugarcane molasses [50], bagasse [51], and corn stalk [52, 53].

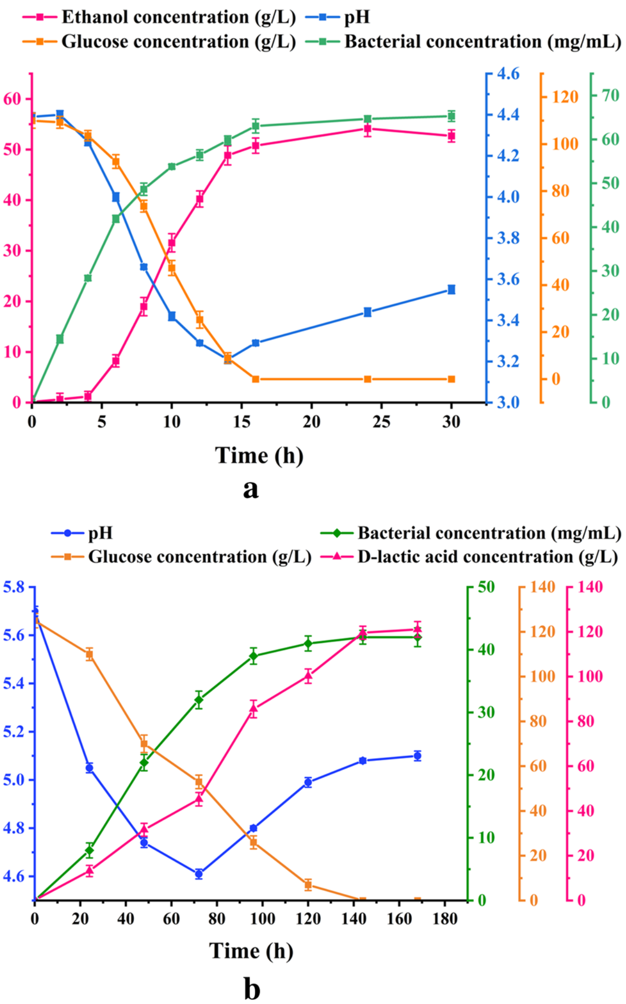

Fig. 4 **a** pH, ethanol, bacterial, and glucose concentrations during ethanol fermentation using the decolorized enzymatic hydrolysate. **b** pH, D-lactic acid, bacterial, and glucose concentrations during D-lactic acid fermentation using the decolorized enzymatic hydrolysate

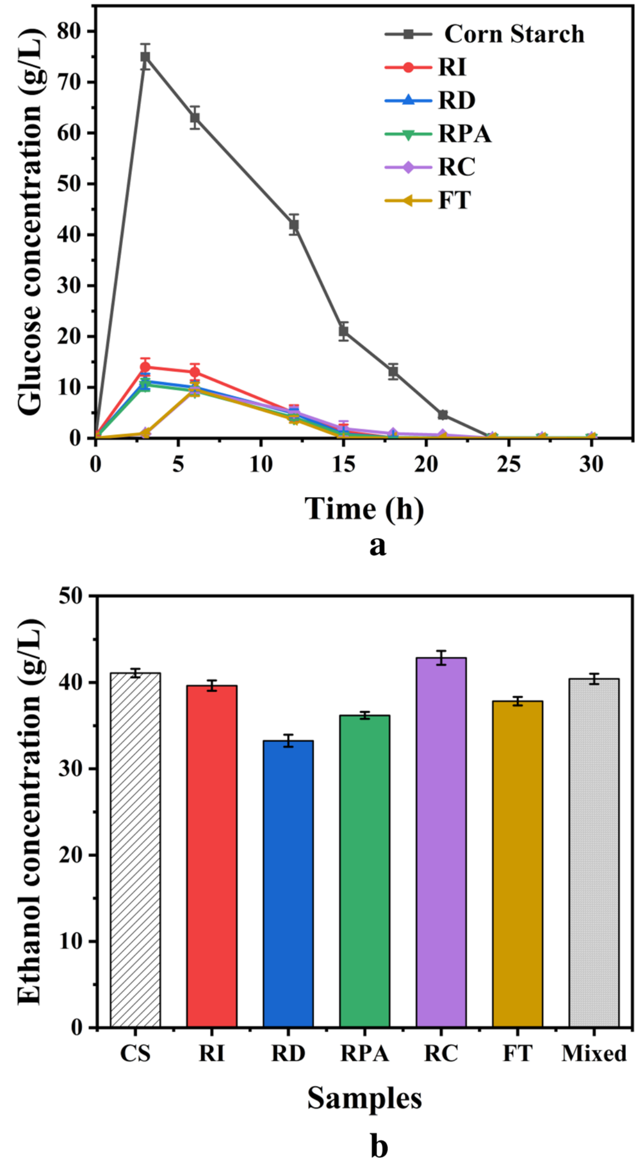

Fig. 5 **a** Glucose concentration during the SSF ethanol process. **b** Maximum ethanol concentration from various TCMDRs via the SSF process

3.3 Preparation of ethanol from starch-rich TCMDRs via the SSF process

Currently, the SSF process, which combines the enzyme-catalyzed conversion of starch into sugar and yeast fermentation of ethanol, is widely used to produce ethanol from starch fermentation [54]. SSF minimizes the inhibition caused by high-glucose concentrations during the initial fermentation stage, shortens the fermentation cycle, and reduces the risk of microbial contamination [55]. In this study, 100 g of corn starch and single or mixed TCMDRs containing 100 g of starch were used as carbon resources to evaluate the feasibility of the SSF ethanol process. The results are presented in Fig. 5a–b.

All starch-rich TCMDRs were suitable for the SSF ethanol process. During the saccharification process (within 6 h), the glucose content of TCMDRs as raw material fluctuated slightly. In contrast, cornstarch exhibited the highest glucose concentration of 75 g/L after 3 h, which was significantly higher than that of single or mixed starch-rich TCMDRs as carbon resources (Fig. 5a). This may be because commercially available corn starch is easily degraded, whereas the starch in TCMDRs is not extracted and tightly bound to lignin and other substances. This resulted in relatively low enzymatic hydrolysis efficiency and stable glucose release and consumption. Except for corn starch, the glucose content of the TCMDRs was reduced to 0 g/L after 21 h. The maximum ethanol concentrations from RI residue, RD residue, RPA residue, RC residue, FT residue, and corn starch as carbon resources

Table 1 Elemental analysis of SSF ethanol process residues SSF

Fermentation residue Samples	N (%)	C (%)	H (%)	S (%)	O (%)	H/C	O/C	(N + O)/C
RI	1.69	38.55	5.94	0.19	42.79	0.15	1.11	1.15
FT	3.01	40.63	6.17	0.32	42.62	0.15	1.05	1.12
RPA	0.74	37.06	5.55	0.06	43.58	0.15	1.18	1.20
RC	3.44	40.30	5.69	0.36	41.08	0.14	1.02	1.10
RD	1.93	38.13	6.01	0.14	42.88	0.16	1.12	1.18

after 24 h were 39.64, 33.25, 36.19, 42.86, 37.84, and 41.09 g/L, respectively (Fig. 5b). The corresponding ethanol yields were 0.40, 0.33, 0.36, 0.43, 0.38, and 0.41 g/g, respectively. Additionally, the ethanol concentration and yield from the mixed TCMDRs as carbon resources reached 40.42 g/L and 0.40 g/g, respectively. Compared to the decolorized enzymatic hydrolysate, TCMDRs exhibited a lower ethanol yield in the SSF process. However, the ethanol yield of starch-rich TCMDRs as feedstock was still higher than that of other reported wastes, such as pomegranate peel (12.9 g/L), coconut shell (8.65 g/L), mango kernel (3.986% v/v) [56–58], and similar to kitchen waste [59, 60]. Therefore, it is feasible to employ starch-rich TCMDRs as feedstocks for biofuel ethanol production using the SSF process, whether in single or mixed forms.

3.4 Preparation of biochar from ethanol fermentation residues

Apart from utilizable starch, TCMDRs also contain non-degraded components such as cellulose, hemicellulose, and lignin, which remain as residues after SSF [61]. After drying, the five types of fermentation residues accounted for 30–50% of the initial weight. The elemental analysis results reveal that C, H, and O were the main components, with contents ranging between 37.06–40.63%, 5.55–6.17%, and 41.08–43.58%, respectively (Table 1). The H/C and O/C ratios of the fermentation residues were 0.14–0.16 and 1.02–1.18, respectively. The infrared spectrum revealed that these residues still contained abundant hydroxyl (3300 cm^{-1}) and carbonyl groups (1700 cm^{-1}) (Fig. 6a). The diffraction peaks at 21.4° observed in the five types of fermentation residues are characteristic of cellulose and hemicellulose (Supplementary information Fig. S3a).

If not handled properly, fermentation residues can impose additional burden on the environment. Carbonization technology is an important method for the waste utilization of fermentation residues, which can eliminate the influence of fermentation residual microorganisms. The obtained biochar can be used in TCM cultivation to increase the content of secondary metabolites in Chinese medicinal materials and alleviate issues related to continuous cropping [62]. Therefore, we used high-temperature carbonization to transform the fermentation residues into biochar (in a tubular furnace at 800 °C for 4 h at a heating rate of 10 °C/min). The yield and elemental analyses of the biochar prepared from the fermentation residue are shown in Table 2. The biochar yields ranged between 23 and 33%. The content of C, O, and H of the biochar produced from various fermentation residues was 77.86–81.29%,

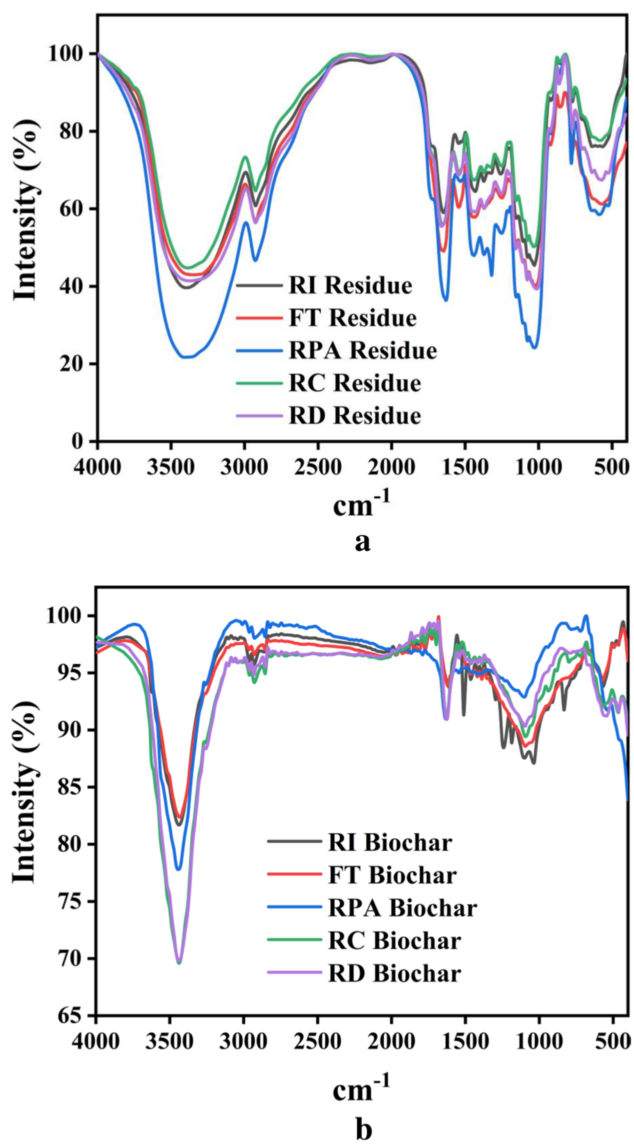

Fig. 6 **a** The FT-IR spectrum of ethanol fermentation residues. **b** The FT-IR spectrum of biochars

Table 2 Elemental analysis of the five types of biochar

Biochar samples	N (%)	C (%)	H (%)	S (%)	O (%)	H/C	O/C	(N + O) /C	Yield(%)
RI	3.26	81.28	0.72	0.17	8.20	0.0089	0.1008	0.1410	25.35
FT	3.82	77.86	0.87	0.09	10.08	0.0128	0.1485	0.2048	29.02
RPA	2.08	78.30	0.66	0.13	8.77	0.0097	0.1284	0.1589	31.75
RC	3.50	79.96	0.69	0.09	7.51	0.0099	0.1073	0.158	33.7
RD	1.58	81.29	1.40	0.15	12.94	0.0228	0.2111	0.2369	23.56

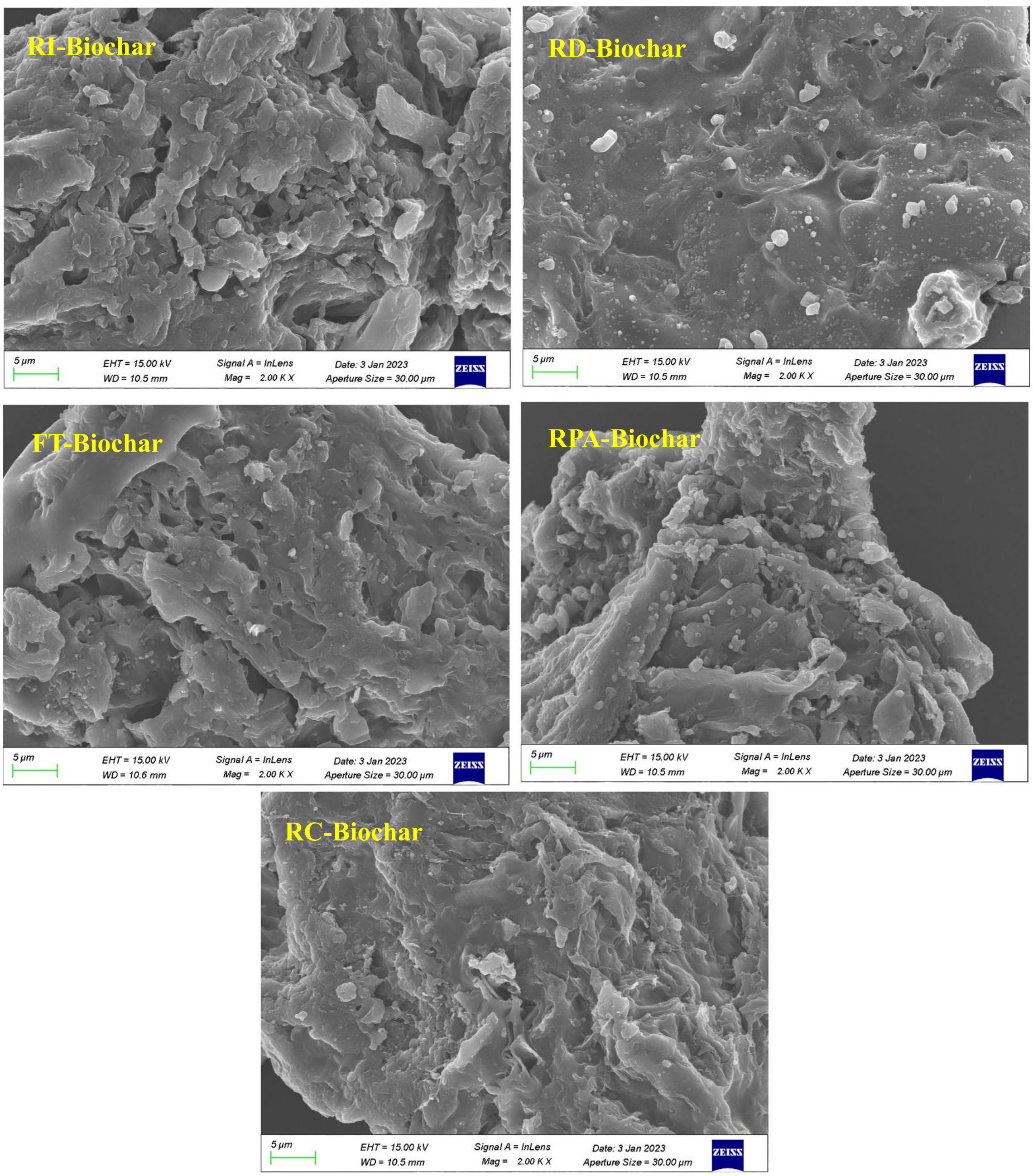

Fig. 7 SEM image of the five types of biochar

Table 3 Pore volume, pore size, and specific surface area of the biochar

Biochar samples	Pore volume (cm^3/g)	Pore size (nm)	Specific surface area (m^2/g)	Reference
RI	0.21	4.91	345.72	--
FT	0.16	5.23	229.97	--
RPA	0.15	5.11	255.56	--
RC	0.16	7.35	89.79	--
RD	0.23	7.81	459.15	--
RI	0.0178	37.23	11.80	[63]
Astragalus	0.187	--	203.70	[64]
Danshen	0.068	3.87	70.3	[65]
Clematis	0.063	7.97	31.74	[66]

8.2–12.94%, and 0.66–1.4%, respectively. The H/C and O/C of the biochar greatly decreased to 0.0089–0.0228 and 0.1008–0.2111, respectively, which indicates that the biochar formed an aromatic structure and its hydrophobicity was enhanced. The infrared spectra also showed that the peaks of the hydroxyl and carbonyl groups were significantly reduced (Fig. 6b). The XRD results showed that the diffraction peak became wider and weaker at 21.4°, and a new diffraction peak appeared at 43.5° after carbonization at high temperatures (Supplementary information Fig. S3b). This was ascribed to the destruction of the microcrystalline structure of cellulose in the fermentation residue after carbonization and the increase in aromatization. The SEM images also show that the biochar had a certain surface concave structure with pore sizes ranging from 1 to 10 μm (Fig. 7).

The pore volume, pore size, and specific surface area of the biochar prepared from the five types of ethanol fermentation residues are listed in Table 3. The specific surface areas of the biochar from the RI, FT, RPA, RC, and RD fermentation residues were 345.72, 229.97, 255.56, 89.79, and 459.15 m^2/g, respectively. In comparison, biochar prepared directly from TCM decoction residues exhibits a low specific surface area [63–66]. Similar to the biochar derived from Danshen residues [65], the specific surface areas, pore volumes, and pore diameters were 70.3m^2/g, 0.068 cm^3/g, and 3.87 nm, respectively. This is mainly because after enzymatic hydrolysis and microbial utilization, the fermentation residue is more conducive to the formation of porous structures. This biochar is expected to have promising applications in soil improvement and sewage adsorption.

4 Conclusion

In conclusion, we propose a comprehensive utilization approach for starch-rich TCMDRs for the production of fermentable sugars via enzymatic hydrolysis, production of ethanol and D-lactic acid via anaerobic fermentation, and generation of biochar from fermentation residue via thermochemical transformation. The glucose yields from both single (RI, RD, RC, FT, and RPA) and mixed starch-rich TCMDRs exceeded 80%. The enzymatic hydrolysates of mixed TCMDRs, after flocculation-decolorization, were used to prepare ethanol and D-lactic acid through anaerobic fermentation, achieving yields close to the theoretical values. Furthermore, when single or mixed starch-rich TCMDRs were directly used as feedstocks for ethanol production via SSF, they exhibited similar ethanol fermentability, with yields ranging from 0.33 to 0.43 g/g. Additionally, by carbonizing the fermentation residue at high temperatures, biochar with a high specific surface area was obtained, which can be applied for pollutant removal, soil improvement, and addressing the challenges of continuous cropping in TCM. This approach will be further applied to the treatment of starch-rich Chinese patent medicine decoction residues, such as Ramuli Cinnamimi and Poriae (Guizhi Fuling).

Supplementary Information The online version contains supplementary material available athttps://doi.org/10.1007/s13399-023-04997-x.

Author contribution XG: methodology, investigation, data curation, writing original draft preparation. TX: data curation, methodology, investigation. YS: investigation. ZB and JZ: formal analysis, data curation. HW: supervising, methodology, funding acquisition, writing (reviewing), and editing. FC: supervising, funding acquisition. PW: conceptualization.

Funding This research was funded by the National Key Research and Development Program of China (2019YFC1906603), the National Natural Science Foundation of China (Grant No. 22078152), and the Jiangsu Synergetic Innovation Center for Advanced Bio-Manufacture (XTD2211).

Data availability It is not applicable.

Declarations

Ethical approval No human and animal studies are in this article.

Competing interests The authors declare no competing interests.

References

1. Yu ZC, Cen YX, Wu BH, Wei C, Xiong F, Li DF, Liu TT, Luo MH, Guo LL, Li YX, Wang LS, Wang JY, Yao J (2019) Berberine prevents stress-induced gut inflammation and visceral hypersensitivity and reduces intestinal motility in rats. World J Gastroenterol 25(29):3956–3971
2. Li T, Peng T (2013) Traditional Chinese herbal medicine as a source of molecules with antiviral activity. Antivir Res 97(1):1–9
3. Huang MY, Zhang LL, Ding J, Lu JJ (2018) Anticancer drug discovery from Chinese medicinal herbs. Chin Med 13:35–44
4. Zhuang TX, Gu XY, Zhou N, Ding LL, Yang L, Zhou MM (2020) Hepatoprotection and hepatotoxicity of Chinese herb Rhubarb

(Dahuang): how to properly control the “General (Jiang Jun)” in Chinese medical herb. Biomed Pharmacother 127:110224
5. Lam P, Cheung F, Tan HY, Wang N, Yuen MF, Feng YB (2016) Hepatoprotective effects of Chinese medicinal herbs: a focus on anti-inflammatory and anti-oxidative activities. Int J Mol Sci 17(4):465–502
6. Fang J, Little PJ, Xu SW (2018) Atheroprotective effects and molecular targets of tanshinones derived from herbal medicine Danshen. Med Res Rev 38(1):201–228
7. Zhi WB, Liu Y, Wang XM, Zhang H (2023) Recent advances of traditional Chinese medicine for the prevention and treatment of atherosclerosis. J Ethnopharmacol 301:115749
8. Yu W, Ilyas I, Aktar N, Xu SW (2022) A review on therapeutical potential of paeonol in atherosclerosis. Front Pharmacol 13:950337
9. Li KJ, Yang HY, Yuan X, Zhang M (2021) Recent developments of heavy metals detection in traditional Chinese medicine by atomic spectrometry. Microchem J 160:105726
10. Tao WY, Jin JJ, Zheng YP, Li S (2021) Current advances of resource utilization of herbal extraction residues in China. Waste and Biomass Valori 12(11):5853–5868
11. Su XY, Xue Q, Sun MC, Liu JR, Wong MH, Wang CX, Chen SL (2021) Co-production of polysaccharides, ginsenosides and succinic acid from Panax ginseng residue: a typical industrial herbal waste. Bioresour Technol 331:125073
12. Zhang S, Chang SY, Xiao P, Qiu SZ, Ye Y, Li LZ, Yan H, Guo S, Duan JN (2019) Enzymatic in *situ* saccharification of herbal extraction residue by a medicinal herbal-tolerant cellulase. Bioresour Technol 287:121417
13. Li YZ, Xu TT, Lin CQ, Xiong H, Bai ZZ, Wu HL, Cao F, Wei P (2022) Determination of lignocellulosic components in traditional Chinese herb residues and its sugar-producing application. Waste and Biomass Valori 14(6):1891–1903
14. Huang C, Li ZX, Wu Y, Huang ZY, Hu Y, Gao J (2021) Treatment and bioresources utilization of traditional Chinese medicinal herb residues: recent technological advances and industrial prospect. J Environ Manag 299:113607
15. De Azevedo ARG, Alexandre J, Pessanha LSP, Manhaes R, De Brito J, Marvila MT (2019) Characterizing the paper industry sludge for environmentally-safe disposal. Waste Manag 95:43–52
16. Cao L, Yu IKM, Tsang DCW, Zhang S, Ok YS, Kwon EE, Song H, Poon CS (2018) Phosphoric acid-activated wood biochar for catalytic conversion of starch-rich food waste into glucose and 5-hydroxymethylfurfural. Bioresour Technol 267:242–248
17. Taskin M, Ortucu S, Unver Y, Arslan NP, Algur OF, Saghafian A (2013) L-lactic acid production by *Rhizopus oryzae* MBG-10 using starch-rich waste loquat kernels as substrate. Staerke 65(3-4):322–329
18. Park JY, Ike M, Arakane M, Shiroma R, Li Y, Arai-Sanoh Y, Kondo M, Tokuyasu K (2011) DiSC (direct saccharification of culms) process for bioethanol production from rice straw. Bioresour Technol 102(11):6502–6507
19. Wang CX, Su XY, Sun W, Zhou SJ, Zheng JY, Zhang MT, Sun MC, Xue JP, Liu X, Xing JM, Chen SL (2018) Efficient production of succinic acid from herbal extraction residue hydrolysate. Bioresour Technol 265:443–449
20. Wang YH, Li SL, Chen IC, Tseng IC, Cheng SS (2010) A study of the process control and hydrolytic characteristics in a thermophilic hydrogen fermentor fed with starch-rich kitchen waste by using molecular-biological methods and amylase assay. Int J Hydrog Energy 35(23):13004–13012
21. Cao LC, Yu IKM, Chen SS, Tsang DCW, Wang L, Xiong XN, Zhang SC, Ok YS, Kwon EE, Song H, Poon CS (2018) Production of 5-hydroxymethylfurfural from starch-rich food waste catalyzed by sulfonated biochar. Bioresour Technol 252:76–82
22. Dutta S, Yu IKM, Fan JJ, Clark JH, Tsang DCW (2022) Critical factors for levulinic acid production from starch-rich food waste: solvent effects, reaction pressure, and phase separation. Green Chem 24(1):163–175
23. Ye X, Shi XY, Xu HX, Feng YQ, Jin BB, Duan PG (2022) Enhanced catalytic activity of layered double hydroxides via in-situ reconstruction for conversion of glucose/food waste to methyl lactate in biorefinery. Sci Total Environ 829:154540
24. Xu TT, Gao X, Li YZ, Lin CQ, Ma PP, Bai ZZ, Zhou J, Wu HL, Cao F, Wei P (2023) Characterization of isolated starch from *Isatis indigotica* Fort. root and anhydro-sugars preparation using its decoction residues. Biomass Convers Biorefin. https://doi.org/10.1007/s13399-023-03892-9
25. Wang Q, Tian D, Hu JG, Huang M, Shen F, Zeng YM, Yang G, Zhang YZ, He JS (2020) Harvesting bacterial cellulose from kitchen waste to prepare superhydrophobic aerogel for recovering waste cooking oil toward a closed-loop biorefinery. ACS Sustain Chem Eng 8(35):13400–13407
26. Weligama Thuppahige VT, Moghaddam L, Welsh ZG, Wang T, Karim A (2023) Investigation of critical properties of Cassava (*Manihot esculenta*) peel and bagasse as starch-rich fibrous agro-industrial wastes for biodegradable food packaging. Food Chem 422:136200
27. Zhang FF, Wang JN, Tian YJ, Liu CX, Zhang SQ, Cao LC, Zhou YM, Zhang SC (2023) Effective removal of tetracycline antibiotics from water by magnetic functionalized biochar derived from rice waste. Environ Pollut 330:121681
28. Xie D, Huang JC, Wang ZQ, Hu W, Liu C, Wang DP, Li X, Qiao Y (2023) Activated carbon derived from hydrochar of food waste for supercapacitor: effect of components on electrochemical performance. Fuel Process Technol 244:107691
29. Sluiter A HB, Ruiz R, Scarlata C, Crocker D (2012) Determination of structural carbohydrates and lignin in biomass. NREL. https://www.nrel.gov/docs/gen/fy13/42618.pdf
30. Din NAS, Lim SJ, Maskat MY, Mohd Zaini NA (2022) Microbial D-lactic acid production, *In Situ* separation and recovery from mature and young coconut husk hydrolysate fermentation broth. Biochem Eng J 188:108680
31. da Silva FL, de Oliveira CA, dos Santos DA, Batista Magalhães ER, de Macedo GR, dos Santos ES (2018) Valorization of an agroextractive residue—Carnauba straw—for the production of bioethanol by simultaneous saccharification and fermentation (SSF). Renew Energy 127:661–669
32. Lin WX, Zhou JL, Sun SY, Yang F, Ye ZW (2022) Optimization of preparation of KOH-modified sludge biochar via response surface method and its enhanced Cd (II) removal from wastewater. Biomass Convers Biorefin. https://doi.org/10.1007/s13399-022-03486-x
33. Cui SB, Zhao Y, Liu YX, Huang RK, Pan JF (2021) Preparation of straw porous biochars by microwave-assisted KOH activation for removal of gaseous H_2S. Energy Fuel 35(22):18592–18603
34. Jia HL, Shi C, Guo JK, Ma PY (2020) Hydrogen sulfide decreases Cd translocation from root to shoot through increasing Cd accumulation in cell wall and decreasing Cd^{2+} influx in Isatis indigotica. Plant Physiol Biochem 155:605–612
35. Sluiter JB, Michel KP, Addison B, Zeng Y, Michener W, Paterson AL, Perras FA, Wolfrum EJ (2021) Direct determination of cellulosic glucan content in starch-containing samples. Cellulose 28(4):1989–2002
36. Sharma D, Saini A (2020) Lignocellulosic ethanol production from a biorefinery perspective: sustainable valorization of waste. Springer Singapore. https://doi.org/10.1007/978-981-15-4573-3_2

37. Seo DJ, Sakoda A (2014) Assessment of the structural factors controlling the enzymatic saccharification of rice straw cellulose. Biomass Bioenergy 71:47–57
38. Ling T, Dempleton WT, Humbird D (2013) Effect of corn stover compositional variability on minimum ethanol selling price (MESP). Bioresour Technol 140:426–430
39. Templeton DW, Wolfrum EJ, Yen JH, Sharpless KE (2016) Compositional analysis of biomass reference materials results from an interlaboratory study. BioEnergy Res 9:303–314
40. Stawski D (2008) New determination method of amylose content in potato starch. Food Chem 110(3):777–781
41. Xu Q (2019) Study on influencing factors of saccharification reaction of corn starch by double enzyme method. J Cereals Oils 32:63–66
42. Chen Y, Krol J, Huang W (2008) Anaerobic yeast fermentation for the production of ethanol in a versatile lab fermentor. Nat Methods. https://doi.org/10.1038/nmeth.f.228
43. Lian TJ, Zhang WQ, Cao QT, Wang SL, Yin FB, Zhou TL, Zhang FY, Dong HM (2023) Efficient production of lactic acid from anaerobic co-fermentation of starch and nitrogen-rich agro-industrial waste using a batch system. Chem Eng J 471:144689
44. Idrees M, Adnan A, Bokhari SA, Qureshi FA (2014) Production of fermentable sugars by combined chemo-enzymatic hydrolysis of cellulosic material for bioethanol production. Braz J Chem Eng 31(2):355–363
45. Chohan NA, Aruwajoye GS, Sewsynker-Sukai Y, Gueguim Kana EB (2020) Valorisation of potato peel wastes for bioethanol production using simultaneous saccharification and fermentation: Process optimization and kinetic assessment. Renew Energy 146:1031–1040
46. Li XJ, Deng YD, Yang Y, Wei ZJ, Cheng JH, Cao LL, Mu DD, Luo SZ, Zheng ZZ, Jiang SJ, Wu XF (2017) Fermentation process and metabolic flux of ethanol production from the detoxified hydrolyzate of cassava residue. Front Microbiol 8:1603–1615
47. Tareen AK, Punsuvon V, Sultan IN, Khan MW, Parakulsuksatid P (2021) Cellulase addition and pre-hydrolysis effect of high solid fed-batch simultaneous saccharification and ethanol fermentation from a combined pretreated oil palm trunk. ACS Omega 6(40):26119–26129
48. Nguyen CM, Choi GJ, Choi YH, Jang KS, Kim J-C (2013) D- and L-lactic acid production from fresh sweet potato through simultaneous saccharification and fermentation. Biochem Eng J 81:40–46
49. Calabia BP, Tokiwa Y (2007) Production of D-lactic acid from sugarcane molasses, sugarcane juice and sugar beet juice by *Lactobacillus delbrueckii*. Biotechnol Lett 29(9):1329–1332
50. Sun YQ, Xu ZZ, Zheng YF, Zhou JJ, Xiu ZL (2019) Efficient production of lactic acid from sugarcane molasses by a newly microbial consortium CEE-DL15. Process Biochem 81:132–138
51. Alves de Oliveira R, Schneider R, Vaz Rossell CE, Maciel Filho R, Venus J (2019) Polymer grade L-lactic acid production from sugarcane bagasse hemicellulosic hydrolysate using *Bacillus coagulans*. Bioresour Techno Reports 6:26–31
52. Wang Y, Meng HY, Cai D, Wang B, Qin PY, Wang Z, Tan TW (2016) Improvement of L-lactic acid productivity from sweet sorghum juice by repeated batch fermentation coupled with membrane separation. Bioresour Technol 211:291–297
53. Liu G, Sun J, Zhang J, Tu Y, Bao J (2015) High titer L-lactic acid production from corn stover with minimum wastewater generation and techno-economic evaluation based on Aspen plus modeling. Bioresour Technol 198:803–810
54. Krajang M, Malairuang K, Sukna J, Rattanapradit K, Chamsart S (2021) Single-step ethanol production from raw cassava starch using a combination of raw starch hydrolysis and fermentation, scale-up from 5-L laboratory and 200-L pilot plant to 3000-L industrial fermenters. Biotechnol Biofuels 14:68–83
55. Ishizaki H, Hasumi K (2014) Ethanol Production from Biomass. Research Approaches to Sustainable Biomass Systems, pp 243–258
56. Mazaheri D, Orooji Y, Mazaheri M, Moghaddam MS, Karimi-Maleh H (2021) Bioethanol production from pomegranate peel by simultaneous saccharification and fermentation process. Biomass Convers Biorefin https://doi.org/10.1007/s13399-021-01562-2
57. Ebrahimi M, Caparanga AR, Villaflores OB (2018) Weak base pretreatment on coconut coir fibers for ethanol production using a simultaneous saccharification and fermentation process. Biofuels 12(3):259–265
58. Awodi PS, Ogbonna JC, Nwagu TN (2022) Bioconversion of mango (*Mangifera indica*) seed kernel starch into bioethanol using various fermentation techniques. Heliyon 8(6):e09707
59. Kim JH, Lee JC, Pak D (2011) Feasibility of producing ethanol from food waste. Waste Manag 31(9-10):2121–2125
60. Singh A, Singhania RR, Soam S, Chen CW, Haldar D, Varjani S, Chang JS, Dong CD, Patel AK (2022) Production of bioethanol from food waste: Status and perspectives. Bioresour Technol 360:127651
61. Lu Q, Li CL (2021) Comprehensive utilization of Chinese medicine residues for industry and environment protection: turning waste into treasure. J Clean Prod 279:123856
62. Sri Shalini S, Palanivelu K, Ramachandran A, Raghavan V (2020) Biochar from biomass waste as a renewable carbon material for climate change mitigation in reducing greenhouse gas emissions—a review. Biomass Convers Biorefin 11(5):2247–2267
63. Yuan HR, Lu T, Wang YZ, Huang HY, Chen Y (2014) Influence of pyrolysis temperature and holding time on properties of biochar derived from medicinal herb (radix isatidis) residue and its effect on soil CO_2 emission. J Anal Appl Pyrolysis 110:277–284
64. Kong XG, Liu YX, Pi JC, Li WH, Liao QTH, Shang JG (2017) Low-cost magnetic herbal biochar: characterization and application for antibiotic removal. Environ Sci Pollut Res Int 24(7):6679–6687
65. Lian F, Sun BB, Song ZG, Zhu LY, Qi XH, Xing BS (2014) Physicochemical properties of herb-residue biochar and its sorption to ionizable antibiotic sulfamethoxazole. Chem Eng J 248:128–134
66. Shen QB, Wang ZY, Yu Q, Cheng Y, Liu ZD, Zhang TP, Zhou SQ (2020) Removal of tetracycline from an aqueous solution using manganese dioxide modified biochar derived from Chinese herbal medicine residues. Environ Res 183:109195